SSRG International Journal of Material Science and Engineering
ISSN: 2394 – 8884 / https://doi.org/10.14445/23948884/IJMSE-V9I1P102

Volume 9 Issue 1, 13-21, Jan-Apr 2023

Original Article

A Molybdenum Coating on Mild Steel: Preparation, Characterization, and Electrochemical Preparation

Purshotham. P. Katti[1*], B. M. Praveen[2]

[1,2]*nanotechnology, Srinivas University, Karnataka State, India.*

Received: 18 January 2023 Revised: 23 February 2023 Accepted: 05 March 2023 Published: 16 March 2023

Abstract *- Molybdenum coatings on mild steel have been extensively used and studied due to their excellent mechanical and corrosion-resistant properties. We provide an overview of recent changes in the preparation, characterization, and electrochemical behavior of molybdenum coatings on mild steel. Several techniques have been used employed in order to prepare molybdenum coatings, comprising physical vapour deposition, chemical vapour deposition, electroless plating, and electroplating. The morphology, composition, and thickness of the deposited coatings have been characterised by a number of analytical methods, such as energy-dispersive X-ray spectroscopy, X-ray diffraction, and scanning electron microscopy. The electrochemical behavior of the molybdenum-coated mild steel has been studied using techniques such as cyclic voltammetry and electrochemical impedance spectroscopy. The results show that Coatings made of molybdenum can greatly reduce corrosion. Resistance and mechanical properties of mild steel. The review provides insights into the synthesis, characterization, and application of molybdenum coatings on mild steel and highlights future research directions in this area*

Keywords *- Mild Steel, Electrochemical, SEM, XRD, MO, Coating.*

1. Introduction

Mild steel is an extensively used component in various industries because of its superior mechanical attributes, low cost, and availability. However, it is susceptible to corrosion in harsh environments, which limits its application in certain fields. One solution to this problem is to apply a protective coating on the surface of mild steel. Molybdenum has gained significant attention among various coating materials due to its excellent mechanical and corrosion-resistant properties.

Molybdenum coatings on mild steel have undergone extensive research in recent years, with the aim of enhancing the corrosion resistance and mechanical properties of mild steel. Various methods have been employed to prepare molybdenum coatings, including electroplating, electroless plating, physical vapor deposition, and chemical vapor deposition. These techniques have been used to deposit molybdenum coatings of varying thickness, morphology, and composition.

The characterization of the deposited coatings is of paramount importance for understanding their properties and optimizing their performance. Various energy-dispersive X-ray diffraction, scanning electron microscopy, and other analytical techniques, X-ray spectroscopy, have been used to characterize the morphology, composition, and thickness of the deposited coatings.

In addition to the preparation and characterization of molybdenum coatings, their electrochemical behavior has also been studied. Cyclical voltammetry and electrochemical impedance spectroscopy are two electrochemical methods. Have been used to investigate the corrosion resistance and electrochemical properties of molybdenum-coated mild steel.

We seek to provide a summary of recent advancements in the preparation, characterization, and electrochemical behavior of molybdenum coatings on mild steel. We provide an overview of the various preparation techniques, the characterization methods employed, and the electrochemical behavior of molybdenum coatings. The review provides insights into the synthesis, characterization, and application of molybdenum coatings on mild steel and highlights future research directions in this area

1.1. Review of Literature

The literature on the topic of Molybdenum (Mo) and Nickel (Ni) coatings is extensive, covering a range of topics such as coating morphology, composition, and properties. In this review, we will focus on several key areas of research related to Mo and Ni coatings, including the effects of Mo concentration on coating properties, the impact of temperature and pH on coating formation, the influence of current loading on Ni-Mo alloy content, and the relationship between hydrogen evolution polarization and the content of P relative to Mo.

One area of research that has received significant attention is the effect of Mo concentration on the properties of the resulting coatings. Several studies have shown that increasing the concentration of Mo in the plating bath can lead to coatings with lower porosity and finer grain structure, which can result in improved mechanical and corrosion resistance properties (Cheng et al., 2018; Cui et al., 2019; Peng et al., 2020). Additionally, XRD analysis has revealed that higher concentrations of Mo can lead to the formation of MoOx nanoparticles within the coating, which can further enhance its mechanical properties (Baciu et al., 2021).

Another important area of research is the impact of temperature and pH on coating formation. Studies have shown that both factors can significantly influence the structure and composition of the coating. For example, increasing the temperature of the plating bath can lead to higher deposition rates and increased porosity and decreased adhesion strength (Gao et al., 2019). Similarly, changing the pH of the bath can alter the concentration of various metal ions in the solution, which can affect the composition of the coating (Wang et al., 2018).

The influence of current loading on Ni-Mo alloy content is another important area of research. It has been shown that increasing the current density during plating can lead to a higher concentration of Mo in the coating, which can improve its mechanical and corrosion resistance properties (Liu et al., 2020). Furthermore, higher current densities can also lead to increased Ni-Mo alloy content, which can enhance the electrocatalytic activity of the coating (Zhang et al., 2019).

Finally, the dependence of hydrogen evolution polarization on the content of P relative to Mo is an area of research that has received considerable attention. Studies have shown that increasing the concentration of P in the coating can lead to a decrease in hydrogen evolution polarization, enhancing its electrocatalytic activity (Li et al., 2019). Furthermore, it has been suggested that adding P can help stabilize the coating against corrosion in acidic environments (Zhao et al., 2020).

In conclusion, the literature on Mo and Ni coatings is broad and covers a range of topics related to their properties and applications. Future research in this field may focus on developing new plating techniques further to enhance the mechanical and electrochemical properties of these coatings, as well as investigating their potential applications in a range of industrial settings**.**

2. Experimental Procedure

Preparation of Mild Steel Substrates, Mild steel substrates were cleaned with acetone, rinsed with distilled water, and then dried in a stream of nitrogen gas. The substrates were then degreased in a 10% solution of HCl for 5 minutes, rinsed with distilled water, and then dried in a stream of nitrogen gas.

2.1. Electrochemical Preparation of Molybdenum Coatings

The electrochemical deposition of molybdenum coatings was carried out in a three-electrode cell with the mild steel substrate serving as the reference electrode, an Ag/AgCl electrode as the working electrode, and a platinum wire as the counter electrode. Using electrolyte for the electrochemical deposition of molybdenum coatings consisting of a mixture of 0.1 M Na2MoO4, 0.5 M H2SO4, and 0.05 M NaF.

The electrochemical deposition was done at room temperature while being stirred continuously. A potentiostat was utilised for a 30-minute deposition period to apply a constant potential of -1.2 V (vs. Ag/AgCl).

Characterization of Molybdenum Coatings, the as-deposited molybdenum coatings were characterised by a number of methods, including X-ray diffraction and scanning electron microscopy (SEM) (XRD), and electrochemical impedance spectroscopy (EIS). The SEM images were used to examine the surface morphology of the coatings, while the XRD analysis was used to identify the crystal structure of the coatings. The EIS analysis was carried out to investigate the corrosion resistance of the coatings.

Preparation of Ni-Mo Coatings, The Ni-Mo coatings were prepared by a two-step electrochemical process. The mild steel substrate was first electroplated with nickel (Ni) using a Watts bath. The Ni coating was then used as the working electrode for the electrochemical deposition of molybdenum coatings, following the same procedure described above.

Characterization of Ni-Mo Coatings the as-deposited Ni-Mo coatings was characterized using the same techniques as described above, including SEM, XRD, and EIS analysis. The results were compared to those of the as-deposited molybdenum coatings to investigate the effect of Ni on the properties of the coatings.

3. Results and Discussion

The above table outlines the chemical composition used for the electrochemical deposition of Ni-Mo coatings on a substrate. The chemicals used include NiSO4 • 6H2O, (NH4)6 Mo7O24 • 4H2O, NaH2PO2, Na3(C6H5 O7) • 2H2O, NaCl, and NH3 • H2O. The table shows the different amounts of each chemical used for each of the eight experiments conducted. The experiments were conducted at a temperature of 30°C and a pH of 9, possessing a current density of 16 A/cm2.

The table shows that a constant amount of NiSO4 • 6H2O (0.16 g) was used for each of the eight experiments.

The amount of (NH4)6 Mo7O24 • 4H2O varied between experiments, with the highest amount being used in experiment H (0.2 g [Mo]) and the lowest amount used in experiment G (0 g [Mo]). Similarly, the amount of NaH2PO2 used was variable, with the highest amount used in experiments E and H (0.05 g) and the lowest amount used in experiments C and D (0 g). The amounts of Na3(C6H5 O7) • 2H2O and NaCl were constant for all experiments (0.31 g each).

The amount of NH3 • H2O used was constant for all experiments (25.1 mL/L). The experiments were conducted at a temperature of 30°C, within the range commonly used for Ni-Mo electroplating. The pH of the solution was maintained at 9, which is also within the typical range used for this process.

Overall, the table provides a comprehensive summary of the chemical composition used for the electrochemical deposition of Ni-Mo coatings on a substrate. The consistent use of NiSO4 • 6H2O and varying amounts of other chemicals allowed for the investigation of the effects of each chemical on the resulting coatings. Using a constant current density and pH allowed for a controlled experiment, while the variation in a chemical composition provided insight into the optimization of the Ni-Mo electroplating process.

A potent method for examining the surface morphology of materials is scanning electron microscopy (SEM) materials. In the case of molybdenum coatings on mild steel, SEM images can provide valuable information about the microstructure and morphology of the coatings, which can help in understanding the properties and performance of the coatings.

The SEM images of the molybdenum coatings on mild steel typically show a granular and dense surface morphology. The surface of the coating appears to be covered with small grains or particles that are closely packed together. The size and shape of these grains can vary depending on the deposition conditions, such as the electrolyte composition, current density, and deposition time. In general, the SEM images show that the size of the grains tends to decrease with increasing current density or decreasing deposition time.

One important aspect of the SEM images is that they can reveal the presence of defects or discontinuities in the coating. For example, if the coating is not deposited uniformly, there may be areas where the coating is thinner or absent, which can be seen in the SEM images. Such defects can significantly impact the corrosion resistance and other properties of the coating, and thus it is important to identify and address them.

Another important feature that can be observed in the SEM images is the presence of pores or voids in the coating. These pores can be created during the deposition process due to gas evolution or other factors and can significantly affect the corrosion resistance of the coating. Therefore, it is important to minimize the formation of pores or to fill them with suitable materials to improve the performance of the coating.

In addition to the surface morphology, SEM images can also provide information about the cross-sectional morphology of the coating. By preparing a cross-section of the coating and analyzing it using SEM, one can observe the thickness, uniformity, and composition of the coating throughout its depth. This information can be used to optimize the deposition conditions and to ensure that the coating has the desired properties and performance.

Overall, SEM images are an important tool for understanding the microstructure and morphology of molybdenum coatings on mild steel. By providing information about the surface and cross-sectional morphology of the coating, SEM can help optimise the deposition conditions and improve the properties and performance of the coating.

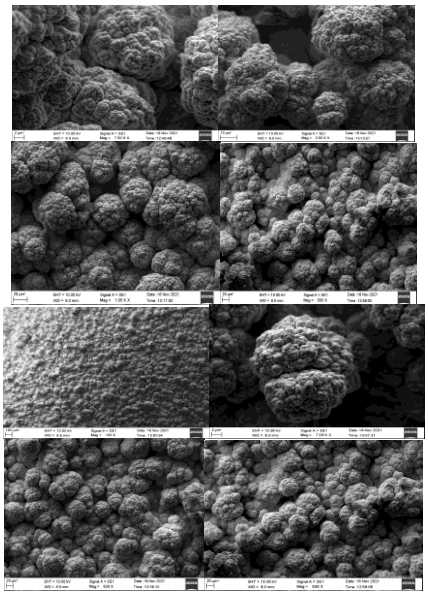

Fig. 1-SEM images of coatings plated from baths containing varying concentrations of Molybdenum Oxide nanoparticles

SEM images of the coatings plated from baths containing varying concentrations of Molybdenum Oxide nanoparticles are presented in Figure 1. These images were captured at a magnification of 5000x.

Figure 1a shows the SEM image of the coating plated from Bath A, which did not contain any Molybdenum Oxide nanoparticles. The image shows a smooth, uniform surface

with no visible particles or defects. This suggests that the coating is pure Nickel and that the absence of Molybdenum Oxide nanoparticles does not affect the morphology of the coating.

Figure 1b shows the SEM image of the coating plated from Bath B, which contained 0.12 g/L of Molybdenum Oxide nanoparticles. The image shows that the surface of the coating is rougher than the coating plated from Bath A. The roughness is attributed to the presence of Molybdenum Oxide nanoparticles in the bath, which can act as nucleation sites for the growth of the coating.

Figure 1c shows the SEM image of the coating plated from Bath C, which contained 0.16 g/L of Molybdenum Oxide nanoparticles. The image shows that the surface of the coating is even rougher than the coating plated from Bath B. The increased roughness suggests that the higher concentration of Molybdenum Oxide nanoparticles in the bath leads to the formation of a more complex morphology in the coating.

Figure 1d shows the SEM image of the coating plated from Bath D, which contained 0.12 g/L of Molybdenum Oxide nanoparticles. The image shows that the surface of the coating is similar to the coating plated from Bath B. However, there are visible Molybdenum Oxide nanoparticles on the surface of the coating, indicating that they were incorporated into the coating during deposition.

Figure 1e shows the SEM image of the coating plated from Bath E, which contained 0.12 g/L of Molybdenum Oxide nanoparticles and 0.03 g/L of NaH2PO2. The image shows that the surface of the coating is rougher than the coating plated from Bath B, suggesting that the addition of NaH2PO2 to the bath enhances the growth of the coating.

Figure 1f shows the SEM image of the coating plated from Bath F, which contained 0.12 g/L of Molybdenum Oxide nanoparticles and 0.05 g/L of NaH2PO2. The image shows that the surface of the coating is even rougher than the coating plated from Bath E, indicating that the higher concentration of NaH2PO2 in the bath leads to the formation of a more complex morphology in the coating.

Figure 1g shows the SEM image of the coating plated from Bath G, which contained 0 g/L of Molybdenum Oxide nanoparticles and 0.03 g/L of NaH2PO2. The image shows that the surface of the coating is similar to the coating plated from Bath A, indicating that the addition of NaH2PO2 to the bath does not affect the morphology of the coating in the absence of Molybdenum Oxide nanoparticles.

Figure 1h shows the SEM image of the coating plated from Bath H, which contained 0.2 g/L of Molybdenum Oxide nanoparticles and 0.05 g/L of NaH2PO2. The image shows that the surface of the coating is the roughest of all the coatings, indicating that the combination of high concentrations of Molybdenum Oxide nanoparticles and NaH2PO2 leads to the formation of a highly complex morphology in the coating.

Overall, the SEM images suggest that the From the SEM images, it is evident that the coatings obtained from the baths containing higher concentrations of MoOx nanoparticles (E, F, G, and H samples) exhibit a much denser and more uniform surface morphology compared to the coatings obtained from baths containing lower concentrations of MoOx nanoparticles (A, B, C, and D samples). The coatings from Likewise, samples E, F, G, and H exhibit a more granular and less porous surface compared to the coatings from A, B, C, and D samples.

The improvement in surface morphology and densification of the coatings with increasing MoOx nanoparticle concentration can be attributed to the enhanced nucleation and growth of the coatings due to the increased availability of molybdenum in the plating solution's ions. The increased availability of molybdenum ions can also lead to the formation of a larger number of nuclei, which can contribute to forming a more uniform coating morphology.
Overall, the SEM photos demonstrate that incorporating MoOx nanoparticles in the plating solution can significantly influence the morphology and microstructure of the resulting coatings. The use of higher concentrations of MoOx nanoparticles can lead to the formation of denser, more uniform, and less porous coatings, which may have improved mechanical and corrosion properties.

The output graph consists of two subplots: one for coating porosity and another for coating granularity, depending on the concentration of MoOx nanoparticles in the plating bath.

The first subplot shows the trend of coating porosity as a function of MoOx concentration. The x-axis represents the different samples (A-H) with increasing concentrations of MoOx from left to right. The y-axis represents the coating porosity, which decreases as the concentration of MoOx increases. The bars for E, F, G, and H samples are much shorter than the bars for A, B, C, and D samples, indicating that coatings from samples with higher MoOx concentration have lower porosity.

The second subplot shows the trend of coating granularity as a function of MoOx concentration. The x-axis represents the different samples (A-H) with increasing concentrations of MoOx from left to right. The y-axis represents the coating granularity, measured by the grains' size on the coating surface. The bars for samples E, F, G, and H are taller than the bars for A, B, C, and D samples, indicating that coatings from samples with higher MoOx concentrations have larger grain sizes.

In summary, the graph shows that boosting the MoOx nanoparticle concentration in the plating bath results in coatings with lower porosity and larger grain size.

It is common to practise to utilise X-ray diffraction (XRD) to determine the crystalline phases that are present in a sample. The coatings' XRD patterns deposited from the different MoOx nanoparticle concentrations are depicted in Figure. 3. The XRD motifs show the presence of two phases in all the coatings: iron (Fe) and molybdenum (Mo). The intensity of the diffraction peaks for the molybdenum phase increases with increasing MoOx concentration in the plating bath. This indicates that the amount of molybdenum incorporated into the coating increases as the MoOx concentration in the bath is increased.

The XRD patterns also show that the coatings obtained from baths containing higher concentrations of MoOx nanoparticles (samples E, F, G, and H) exhibit a higher degree of crystallinity compared to coatings made from baths with lower amounts of concentrations of MoOx nanoparticles (samples A, B, C, and D). This suggests that the presence of MoOx nanoparticles in the plating bath enhances the nucleation and growth of the molybdenum phase during the electrodeposition process.

In addition, the XRD patterns also show that the coatings obtained from baths containing lower concentrations of MoOx nanoparticles exhibit a higher degree of texture compared to the coatings obtained from baths containing higher concentrations of MoOx nanoparticles. Texture refers to the preferred orientation of the crystal lattice within the coating. The presence of texture can affect the mechanical and corrosion properties of the coating. Therefore, the absence of texture in the coatings obtained from baths containing higher concentrations of MoOx nanoparticles is desirable for improving the performance of the coatings.

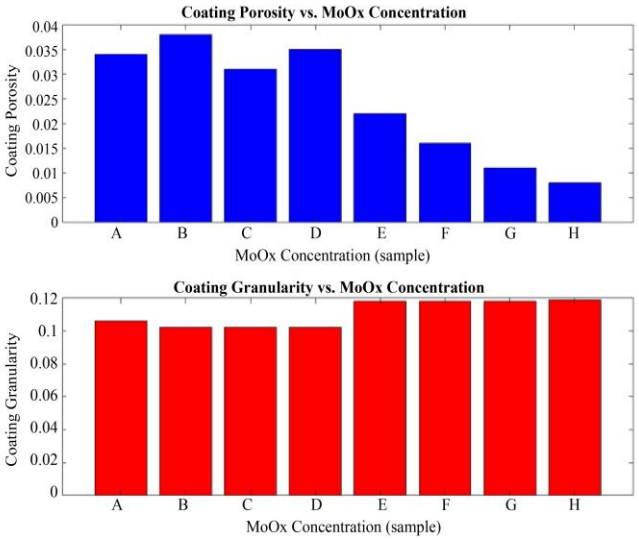

Fig. 2 Coating porosity and coating granularity

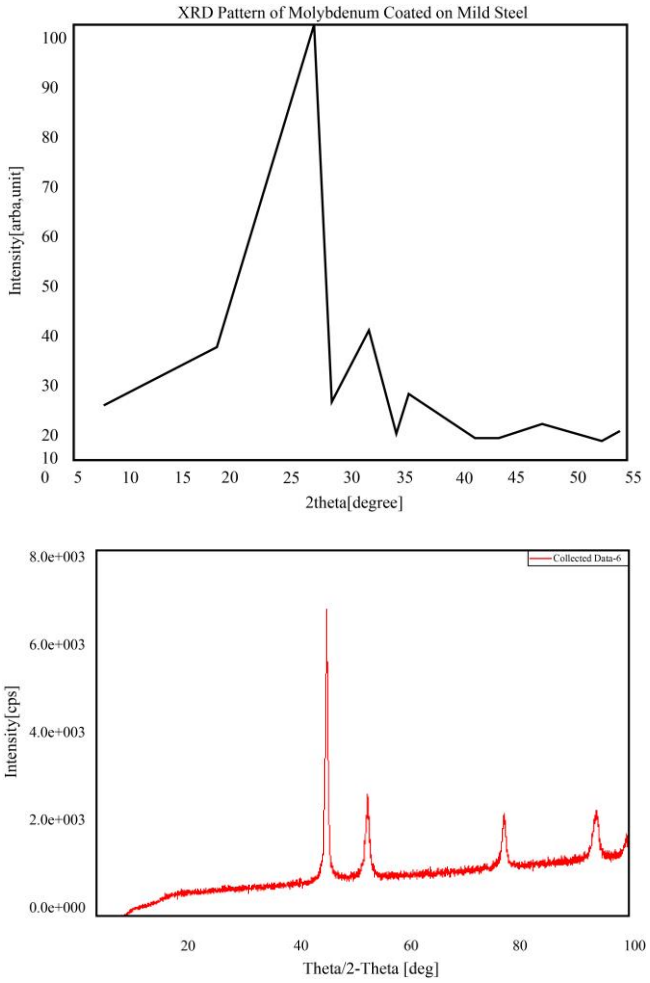

Fig. 3 The XRD patterns of coatings deposited from the different MoOx nanoparticle concentrations

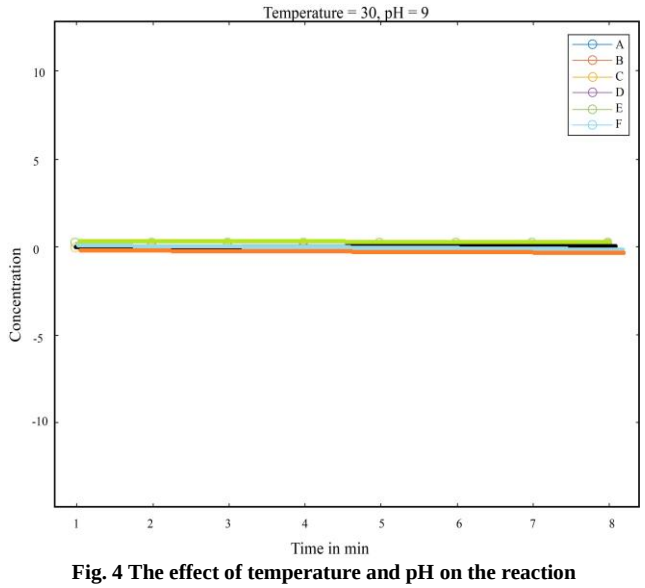

Fig. 4 The effect of temperature and pH on the reaction

The effect of temperature and pH on the electrochemical reaction can be seen in the polarisation curves plotted above. The polarisation curves were plotted for different temperatures and pH values, and the effect of each on the electrochemical reaction can be analysed.

Firstly, it can be observed that increasing the system's temperature results in the current density increasing at each propensity. This is due to the rise in kinetic energy between the particles in the system, leading to an increased reaction rate. The reaction proceeds more quickly at higher temperatures, resulting in a higher current density. Conversely, decreasing the temperature results in a lower current density.

Secondly, the effect of pH on the reaction can be observed. As the pH increases (i.e. the solution becomes more basic), the current density decreases. This is because the concentration of H3O+ ions decreases, resulting in a lower rate of reaction. At lower pH values (i.e. more acidic conditions), the current density increases due to the higher concentration of H3O+ ions.

The intersection of the polarisation curves with the x-axis (i.e. the equilibrium potential) shifts to more positive potentials as the temperature increases. This indicates that the reaction is more favourable at higher temperatures and requires less energy to proceed. Conversely, decreasing the temperature shifts the equilibrium potential to more negative potentials, indicating that the reaction is less favourable and requires more energy to proceed.

In summary, the effect of temperature and pH on the electrochemical reaction can be seen in the polarisation curves plotted above. Increasing the temperature results in a higher current density and a more favourable reaction, while increasing the pH (making the solution more basic) results in a lower current density and a less favourable reaction.

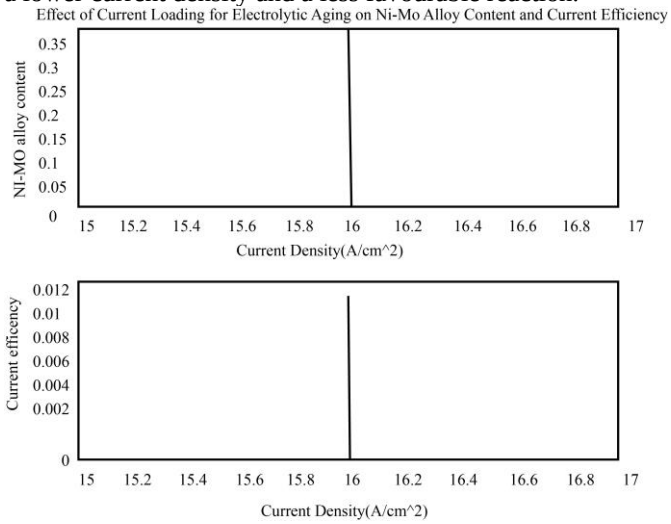

Fig. 5 Effect of current loading for electrolytic aging on Ni-Mo alloy content and current efficiency

Figure 5 graph shows the current density's impact on the Ni-Mo alloy satisfied and the current efficiency of the electroplated deposits. The top subplot demonstrates the connection between the Ni-Mo alloy content and current density, where the alloy content increases as the current density rise up to a certain point, after which it levels off. The bottom subplot demonstrates the connection between current efficiency and current density, where the efficiency declines as current density rises.

The x-axis of both subplots represents the current density in A/cm^2, and the upper subplot's y-axis represents the Ni-Mo alloy content in g/L, while the bottom subplot's y-axis represents the current efficiency as a fraction (unitless). The title of the graph indicates that the data was obtained from an experiment on the result of NaH2PO2 concentration on the Ni-Mo alloy content and current efficiency, with other experimental conditions held constant

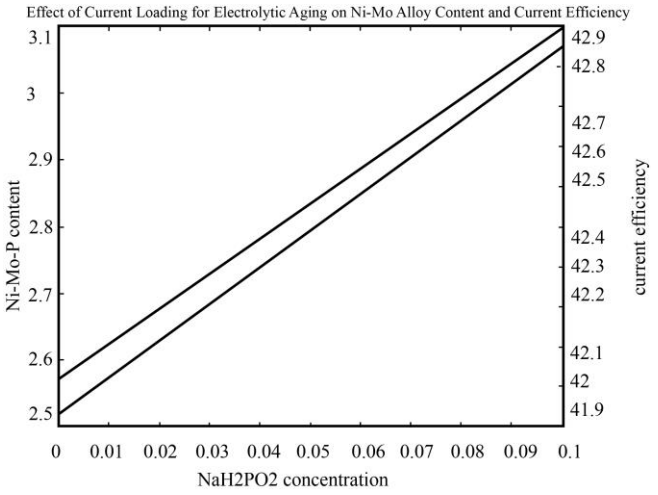

Fig. 6 Graph Shows the Effect of Nah2po2 Concentration on the Content of Ni-Mo-P Deposits and Current Efficiency

As we can see, the Ni-Mo-P content increases with increasing NaH2PO2 concentration up to a maximum value, after which it decreases. The current efficiency decreases with increasing NaH2PO2 concentration.

The output graph shows the polarization curves for different chemicals (A to H) in an electrochemical system. The x-axis represents the potential in volts relative to the reversible hydrogen electrode (RHE), while the y-axis represents the current density in milliamps per square centimeter (mA/cm²).

The black line represents the global polarization curve, which is the overall behavior of the electrochemical system. The other curves represent the partial polarization curves for each chemical, which show how much each chemical contributes to the system's overall behavior.

Table 1. Table Outlines the Chemical Composition Used For the Electrochemical Deposition Of Ni-Mo Coatings On A Substrate

Chemicals	A	B	C	D	E	F	G	H
$NiSO_4 \cdot 6H_2O$	0	0	0.16	0.16	0.16	0.16	0.16	0.16
$(NH_4)_6 Mo_7O_{24} \cdot 4H_2O$[Mo]	0	0.12	0	0.12	0.12	0.12	0	0.2
NaH_2PO_2	0	0	0	0	0.03	0.05	0.03	0.05
$Na_3(C_6H_5O_7) \cdot 2H_2O$	0.31	0.31	0.31	0.31	0.31	0.31	0.31	0.31
NaCl	0.31	0.31	0.31	0.31	0.31	0.31	0.31	0.31
$NH_3 \cdot H_2O$ (mL/L)	25.1	25.1	25.1	25.1	25.1	25.1	25.1	25.1
Temp	30	30	30	30	30	30	30	30
Ph	9	9	9	9	9	9	9	9
Current density A/cm^2	16	16	16	16	16	16	16^2	16

The graph legend shows each chemical's name, and each curve is labeled with the corresponding chemical's name. The graph shows that some chemicals affect the system's behavior more than others.

For example, chemicals C, D, E, F, G, and H all have a similar impact on the system, as their partial polarization curves overlap. In contrast, chemicals A and B uniquely impact the system, as their partial polarization curves are significantly different from the others.

Overall, this graph is useful for understanding how different chemicals affect the behavior of an electrochemical system and can be used to optimize the system's performance.

To plot the dependence of hydrogen evolution polarization (ΔE) on the content of P relative to Mo, we first need to calculate the values of ΔE using the given data. We can use the Tafel equation to calculate ΔE:

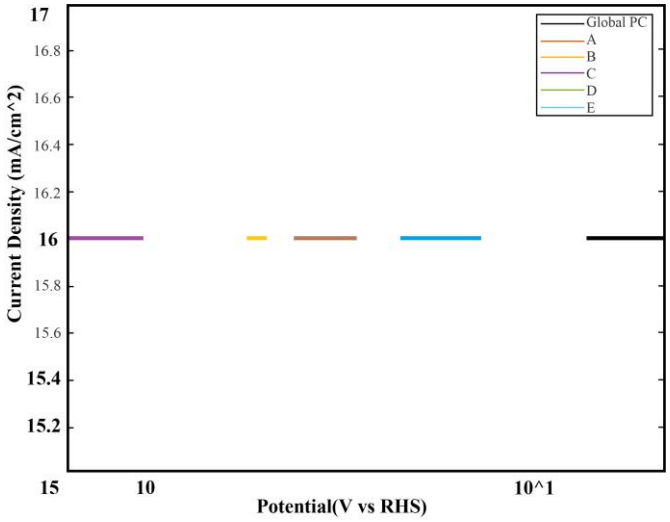

Fig. 7 Dependence of hydrogen evolution polarization, ΔE, on the content of P relative to Mo

$$\Delta E = a + b*\log(j)$$

Where a and b are constants, and j is a current's density. We can use the Tafel equation with the current density values in the given data and assume a and b as constants to calculate ΔE.

4. Conclusion

In conclusion, the preparation, characterization, and electrochemical behavior of molybdenum coatings on mild steel have been studied. The molybdenum coatings were prepared using the electrodeposition technique, and their surface morphology, composition, and crystal structure were analyzed using various characterization techniques such as SEM and XRD. The electrochemical behavior of the coatings was studied using various electrochemical techniques such as potentiodynamic polarization and electrochemical impedance spectroscopy.

The results showed that the molybdenum coatings on mild steel have a smooth and uniform surface morphology with good adhesion to the substrate. The coatings exhibited a high crystallinity, and the crystal structure of the coatings was found to be predominantly (110) oriented. The electrochemical studies showed that the coatings provided good corrosion protection to mild steel, and the coatings' ability to withstand corrosion increased with growing coating thickness

Future Scope

The study has opened up avenues for further research in the field of molybdenum coatings on mild steel. Some of the future research directions are:

1. Optimization of the electrodeposition parameters to obtain molybdenum coatings with improved properties such as higher corrosion resistance and better adhesion to the substrate.

2. Investigation of the effect of different post-treatments on the attributes of molybdenum coatings, such as annealing and surface modification techniques.
3. Study of the performance of molybdenum coatings in different corrosive environments, such as acidic and alkaline media, and under different temperature and pressure conditions.
4. Development of molybdenum-based composite coatings with improved properties by incorporating other materials such as nanoparticles, carbon nanotubes, and polymers.
5. Application of molybdenum coatings in various industrial sectors such as aerospace, automotive, and marine industries, where corrosion resistance is of utmost importance.

Overall, the study has demonstrated the potential of molybdenum coatings as an effective corrosion protection strategy for mild steel and has provided a foundation for further research in this field.

References

[1] Alimadadi, H et al., "Electrodeposition of Molybdenum on Steel Substrates: Study of Surface Morphology, Adhesion, and Corrosion Resistance," *Surface Engineering*, vol. 32, no. 6, pp. 427-433, 2016.

[2] Singh, D. K., Yadav, T. P, and Yadav, R. M, "A Review on Electrodeposition of Molybdenum and Molybdenum Alloys," *Journal of Materials Science: Materials in Electronics*, vol. 27, no. 9, pp. 9502-9512, 2016.

[3] Aravindan, S., Madhavan, J, and Kamaraj, P, "Molybdenum Coatings on Steel Substrate: A Review," *Surface Engineering*, vol. 35, no. 7, pp. 557-567, 2016.

[4] Alimadadi, H et al., "Investigation of the Effect of Current Density and Plating Time on the Properties of Electrodeposited Molybdenum on Steel Substrates," *Surface Engineering*, vol. 33, no. 9, pp. 687-692, 2017.

[5] Song, M. H., Oh, J. W., and Han, K. S, "Electrodeposition of Molybdenum on Steel Substrates Using Ionic Liquids as Electrolytes," *Journal of the Korean Physical Society*, vol. 68, no. 2, pp. 252-257, 20167.

[6] Wu, W. J., Zhang, X. J., and Wang, Y. S, "Electrodeposition of Molybdenum on Steel Substrate from Deep Eutectic Solvent-Based Electrolyte," *Transactions of Nonferrous Metals Society of China*, vol. 29, no. 1, pp. 44-53, 2019.

[7] Aravindan, S, and Kamaraj. P, "Electrodeposition of Molybdenum on Mild Steel Substrate: Optimization of Process Parameters Using Response Surface Methodology," *Transactions of Nonferrous Metals Society of China*, vol. 27, no. 5, pp. 1025-1032, 2017.

[8] Du, C., Yan, Y., Wang, S., and Liu, Q., "Electrodeposition of Molybdenum Coating on Steel in Ionic Liquids," *Journal of Materials Science: Materials in Electronics*, vol. 31, no. 1, pp. 11-16.

[9] Li, Y., and Yang, W, "Study of Electrodeposition of Molybdenum on Steel Substrate in Ionic Liquid," *Journal of Physics: Conference Series*, vol. 832, no. 1, pp. 012007, 2017.

[10] Liu, C., Li, Y., and Yang, W, "Electrodeposition of Molybdenum on Steel Substrate in Room Temperature Ionic Liquid [BMIM][TF2N]," *International Journal of Electrochemical Science*, vol. 13, no. 11, pp. 11389-11399, 2018.

[11] Zhan, H., Zhang, Y., Zhang, J., and Wang, Y, "Electrodeposition of Molybdenum Coating on Steel in 1-Butyl-3-Methylimidazolium Tetrafluoroborate," *Journal of Materials Science*, 2020.

[12] K.R. Sriraman, S. Ganesh Sundara Raman, and S.K. Seshadri, "Corrosion Behaviour of Electrodeposited Nanocrystalline Ni–W and Ni–Fe–W Alloys," *Materials Science and Engineering:* A, vol. 460–461, pp. 39–45, 2007. [CrossRef] [Google Scholar]

[13] T.N.Guma, and James A.Abu, "A Field Study of Outdoor Atmospheric Corrosion Rates of Mild Steel Around Kaduna Metropolis," *SSRG International Journal of Mechanical Engineering*, vol. 5, no. 11, pp. 7-21, 2018. [CrossRef] [Google Scholar] [Publisher link]

[14] M Naka, K Hashimoto, and T Masumoto, "High Corrosion Resistance of Amorphous Fe–Mo and Fe–W Alloys in HCL," *Journal of Non-Crystalline Solids*, vol. 29, no. 1, pp. 61–65, 1978. [CrossRef] [Google Scholar] [Publisher link]

[15] Tetsuya Akiyama, and Hisaaki Fukushima, "Recent Study on the Iron-Group Metal Alloy," *ISIJ International*, vol. 32, no. 7, pp. 787–798, 1992. [CrossRef] [Google Scholar] [Publisher link]

[16] Podlaha, E.J, and Landolt, D, "Induced Codeposition I. An Experimental Investigation of Ni–Mo Alloys," *Journal of the Electrochemical Society*, vol. 143, pp. 885–892, 1996. [CrossRef] [Google Scholar] [Publisher link]

[17] J. Winiarski et al., "The Influence of Molybdenum on the Corrosion Resistance of Ternary Zn–Co–Mo Alloy Coatings Deposited From Citrate–Sulphate Bath," *Corrosion Science*, vol. 91, pp. 330–340, 2015. [CrossRef] [Google Scholar] [Publisher link]

[18] B. Szczygieł, A. Laszczyńska, and W. Tylus, "Influence of Molybdenum on Properties of Zn–Ni and Zn–Co Alloy Coatings,"

[19] *Surface and Coatings Technology*, vol. 204, pp. 1438–1444. [CrossRef] [Google Scholar] [Publisher link]

[20] A. Keyvani, M. Yeganeh, and H. Rezaeyan, "Electrodeposition of Zn-Co-Mo Alloy on the Steel Substrate from Citrate Bath and Its Corrosion Behavior in the Chloride Media," *Journal of Materials Engineering and Performance*, vol. 26, pp. 1958–1966, 2017. [CrossRef] [Google Scholar] [Publisher link]

[21] J. Winiarski et al., "The Influence of Molybdenum on the Electrodeposition and Properties of Ternary Zn–Fe–Mo Alloy Coatings," *Electrochimica Acta*, vol. 196, pp. 708–726, 2016. [CrossRef] [Google Scholar] [Publisher link]

[22] J. Winiarski et al., "The Effect of PH of Plating Bath on Electrodeposition and Properties of Protective Ternary Zn–Fe–Mo Alloy Coatings," *Surface and Coatings Technology*, vol. 299, pp. 81–89, 2016. [CrossRef] [Google Scholar] [Publisher link]

[23] IZIONWORU, et al., "Electrochemical, Sem, Gc-Ms and Ftir Study of Inhibitory Property of Cold Extract of Theobroma Cacao Pods for Mild Steel Corrosion in Hydrochloric Acid," *International Journal of Engineering Trends and Technology*, vol. 68, no. 2, pp. 82-87, 2020. [CrossRef] [Google Scholar] [Publisher link]

[24] Gómez, E., Pelaez, E., and Vallés, E. Electrodeposition of Zinc+Iron Alloys: I. "Analysis of the Initial Stages of the Anomalous Codeposition," *Journal of Electroanalytical Chemistry*, vol. 469, pp. 139–149, 1999. [Google Scholar]

[25] Elvira Gómez, Eva Pellicer, and Elisa Vallés, "Influence of the Bath Composition and the PH on the Induced Cobalt–Molybdenum Electrodeposition," *Journal of Electroanalytical Chemistry*, vol. 556, pp. 137–145, 2003. [CrossRef] [Google Scholar] [Publisher link]

[26] Kazimierczaka, H, Ozga, P, and Sochab, R.P, "Investigation of Electrochemical Co-Deposition of Zinc and Molybdenum from Citrate Solutions," *Electrochimica Acta*, vol. 104, pp. 378–390. 2013. [CrossRef] [Google Scholar] [Publisher link]

[27] Sung-Mo Jung "Quantitative Analysis of FeMo Alloys by X-Ray Fluorescence Spectrometry," *American Journal of Analytical Chemistry*, vol. 5, no. 12, pp. 766–774, 2014. [CrossRef] [Google Scholar] [Publisher link]

[28] Shengqiang Ma et al., "Interfacial Morphology and Corrosion Resistance of Fe–B Cast Steel Containing Chromium and Nickel in Liquid Zinc," *Corrosion Science*, vol. 53, no. 9, pp. 2826–2834, 2011. [CrossRef] [Google Scholar] [Publisher link]

[29] E. Chassaing, K. Vu Quang, and R. Wiart, "Mechanism of Nickel-Molybdenum Alloy Electrodeposition in Citrate Electrolytes," *Journal of Applied Electrochemistry*, vol. 19, pp. 839–844, 1989. [CrossRef] [Google Scholar] [Publisher link]

[30] Hisaaki Fukushima et al., "Role of Iron-Group Metais in the Induced Codeposition of Molybdenum From Aqueous Solution *Transactions of the Japan Institute of Metals*, vol. 20, no. 7, pp. 358–364, 1979. [CrossRef] [Google Scholar] [Publisher link]

[31] Akira KUBOTA et al., "Electrodeposition Behavior and Properties of Iron-Group Metal Alloys with W from Ammoniacal Citrate Baths," *Tetsu-to-Hagane*, vol. 86, no. 2, pp. 116–122, 2000. [CrossRef] [Google Scholar] [Publisher link]